

# CrystEngComm

Accepted Manuscript



This is an *Accepted Manuscript*, which has been through the Royal Society of Chemistry peer review process and has been accepted for publication.

*Accepted Manuscripts* are published online shortly after acceptance, before technical editing, formatting and proof reading. Using this free service, authors can make their results available to the community, in citable form, before we publish the edited article. We will replace this *Accepted Manuscript* with the edited and formatted *Advance Article* as soon as it is available.

You can find more information about *Accepted Manuscripts* in the [Information for Authors](#).

Please note that technical editing may introduce minor changes to the text and/or graphics, which may alter content. The journal's standard [Terms & Conditions](#) and the [Ethical guidelines](#) still apply. In no event shall the Royal Society of Chemistry be held responsible for any errors or omissions in this *Accepted Manuscript* or any consequences arising from the use of any information it contains.

# Controlled synthesis of bismuth-containing compounds ( $\alpha$ , $\beta$ and $\delta$ - $\text{Bi}_2\text{O}_3$ , $\text{Bi}_5\text{O}_7\text{NO}_3$ and $\text{Bi}_6\text{O}_6(\text{OH})_2(\text{NO}_3)_4 \cdot 2\text{H}_2\text{O}$ ) and their photocatalytic performance†

Shu Gong, Qiaofeng Han<sup>\*</sup>, Xin Wang, and Junwu Zhu<sup>\*</sup>

**Abstract:** Basic bismuth nitrate ( $\text{Bi}_6\text{O}_6(\text{OH})_2(\text{NO}_3)_4 \cdot 2\text{H}_2\text{O}$ ; BiON),  $\alpha$  and  $\delta$ - $\text{Bi}_2\text{O}_3$ , or  $\text{Bi}_5\text{O}_7\text{NO}_3$  and  $\beta$ - $\text{Bi}_2\text{O}_3$  were synthesized from  $\text{Bi}(\text{NO}_3)_3 \cdot 5\text{H}_2\text{O}$  using a facile solution crystallization route or subsequent calcination procedure by adjusting growth parameters such as a base and solvent. When using hexamethylenetetramine (HMT) as a base, the distorted hexagonal BiON prisms could be prepared in a mixed solution of 2-methoxyethanol (EM) and  $\text{H}_2\text{O}$  (pH range 2.5-6), whereas  $\delta$ - $\text{Bi}_2\text{O}_3$  nanosheets were obtained if using ethylene glycol (EG) instead of EM (pH  $\approx$  6). The addition of  $\text{NH}_3 \cdot \text{H}_2\text{O}$  as a base gave birth to amorphous nanoparticles in EG- $\text{H}_2\text{O}$  (pH  $\approx$  6) and EM- $\text{H}_2\text{O}$  (pH range 6-9) solution, or amorphous nanotubes in  $\text{H}_2\text{O}$  (pH  $\approx$  9) solution, which completely converted to well-crystalline  $\beta$ - $\text{Bi}_2\text{O}_3$  nanoparticles or  $\text{Bi}_5\text{O}_7\text{NO}_3$  nanoplates through calcination at 300, 350 and 400 °C for 2 h, respectively. Analogous to previous work, NaOH as a base in  $\text{H}_2\text{O}$  or NaOH/EM- $\text{H}_2\text{O}$  solution (pH > 13) induced the formation of  $\alpha$ - $\text{Bi}_2\text{O}_3$ . The studies of the photocatalytic activity of the as-prepared samples indicated that  $\delta$ - $\text{Bi}_2\text{O}_3$  nanosheets and  $\text{Bi}_5\text{O}_7\text{NO}_3$  nanoplates exhibited the highest degradation efficiency for Rhodamine (RhB) under visible light irradiation owing to their sheet or plate-like morphology and the associated high surface areas.

**Keywords:** Bismuth-based compounds; Solution crystallization;

Micro/nanostructures; Photocatalysis

## 1. Introduction

Developing visible-light driven photocatalysts for pollutants degradation is of great values for environmental remediation and solar energy utilization. Various bismuth-based compounds such as  $\text{Bi}_2\text{O}_3$ ,<sup>1,2</sup>  $\text{BiOX}$  ( $X = \text{Cl}, \text{Br}, \text{I}$ ),<sup>3</sup>  $(\text{BiO})_2\text{CO}_3$ <sup>4</sup> and so on, have recently attracted more consideration because of their potential application as photocatalysts in water splitting and contaminants decomposition. Of these compounds,  $\text{Bi}_2\text{O}_3$  is the simplest and most significant bismuth oxide, which has been suggested to be a suitable photocatalyst owing to its relatively smaller band gap, higher oxidation power of the valence hole and non-toxicity.<sup>5</sup>  $\text{Bi}_2\text{O}_3$  has four main polymorphs labeled as  $\alpha$ ,  $\beta$ ,  $\gamma$  and  $\delta$ - $\text{Bi}_2\text{O}_3$ , which possesses excellent electrical, optical, photocatalytic and conducting properties.<sup>6</sup> Thanks to their phases, shapes and sizes-dependent properties, controlled synthesis of  $\text{Bi}_2\text{O}_3$  nanocrystals with well-defined morphology and polymorph not only benefits fundamental research but also offers great promise for practical application.<sup>7</sup> There have been many papers on morphology and polymorph-tuned preparation of  $\text{Bi}_2\text{O}_3$  nanocrystals. For example, Lu et al. reported the synthesis of bouquet-like  $\alpha$ - $\text{Bi}_2\text{O}_3$  via a hydrothermal method by the synergistic control of NaOH and polyvinyl alcohol.<sup>8</sup> Three-dimensional (3D) flower-like  $\alpha$ - $\text{Bi}_2\text{O}_3$  microstructures have been synthesized via solution precipitation by Wang's group and our work.<sup>9,10</sup> Yu et al. prepared  $\alpha$  and  $\beta$ - $\text{Bi}_2\text{O}_3$  hierarchical structures via a precursor-induced synthesis by using a hydrothermal technique and subsequent calcination.<sup>11</sup> Monodispersed  $\beta$ - $\text{Bi}_2\text{O}_3$  nanospheres were synthesized by

D-fructose assisted solvothermal and calcining process.<sup>12</sup> Nan's group prepared  $\beta$ - $\text{Bi}_2\text{O}_3$  and  $\beta$ - $\text{Bi}_2\text{O}_3$ / $(\text{BiO})_2\text{CO}_3$  microspheres through the thermal decomposition of  $(\text{BiO})_2\text{CO}_3$ .<sup>13</sup> Chen et al. prepared  $\beta$ - $\text{Bi}_2\text{O}_3$  nanotubes in EG solution through a solvothermal route.<sup>14</sup>  $\beta$ - $\text{Bi}_2\text{O}_3$  nanotubes arrays were obtained through self-sacrificing route by the oxidization of metallic bismuth nanotubes.<sup>15</sup> By contrast, there have been only a couple of reports on the synthesis of  $\delta$ - $\text{Bi}_2\text{O}_3$ . Wang et al synthesized  $\delta$ - $\text{Bi}_2\text{O}_3$  hierarchical nanostructures in the presence of  $\text{VO}_3^-$  at 60-80 °C and studied its photocatalytic activity for Rhodamine (RhB) degradation.<sup>16</sup> Yang's group prepared microsette-like  $\delta$ - $\text{Bi}_2\text{O}_3$  by a hydrothermal route, which exhibited selective capture of iodide from solutions.<sup>17</sup> Most of these synthetic processes required surfactants or hydrothermal treatment, which may impede scale-up production for application due to tedious removal procedure of the surfactants and energy consumption. Besides, one synthetic protocol could lead to  $\text{Bi}_2\text{O}_3$  with only one or two polymorphs. The oriented synthesis of the target structures of  $\text{Bi}_2\text{O}_3$  is of great significance for both materials synthesis and application. To the best of our knowledge, no systematic investigation on the phase- and shape-controlled synthesis of  $\text{Bi}_2\text{O}_3$  nanoparticles has been carried out by a facile solution crystallization route. In this work,  $\text{Bi}_2\text{O}_3$  with  $\alpha$ ,  $\beta$  and  $\delta$  phase have been fabricated from the precursor  $\text{Bi}(\text{NO}_3)_3 \cdot 5\text{H}_2\text{O}$  by tuning growth parameters. The results reveal that the nature of solvents (2-methoxyethanol (EM), ethylene glycol (EG) and  $\text{H}_2\text{O}$ ) and bases (hexamethylenetetramine (HMT), ammonia ( $\text{NH}_3 \cdot \text{H}_2\text{O}$ ) and NaOH) plays a crucial role in the phase and shape of the final products. Among the as-prepared bismuth trioxides,  $\delta$ - $\text{Bi}_2\text{O}_3$  nanosheets possessed the highest visible light

driven photocatalytic activity for RhB degradation. Besides, as an efficient visible light active catalyst,  $\text{Bi}_5\text{O}_7\text{NO}_3$  could be prepared from the calcination of the precursor obtained from the reaction of  $\text{Bi}(\text{NO}_3)_3$  and  $\text{NH}_3 \cdot \text{H}_2\text{O}$  aqueous solution.

Furthermore, bismuth nitrate pentahydrate ( $\text{Bi}(\text{NO}_3)_3 \cdot 5\text{H}_2\text{O}$ ) is known as a compound which is hydrolyzed with water into basic bismuth nitrates with many complicated compositions  $[\text{Bi}_6\text{O}_{4+x}(\text{OH})_{4-x}(\text{NO}_3)_{(6-x)} \cdot n\text{H}_2\text{O}]$ ,  $x = 0 - 2$ ;  $n = 0 - 3$ .<sup>18</sup> These basic nitrates could be used as a mild antiseptic and potential photocatalysts.<sup>19,20</sup> In order to obtain phase pure product, hydrolysis reaction with alkaline was proceeded under hydrothermal condition or ambient condition by finely tuning pH of solution.<sup>18,19</sup> Herein, phase pure  $\text{Bi}_6\text{O}_6(\text{OH})_2(\text{NO}_3)_4 \cdot 2\text{H}_2\text{O}$  (denoted as BiON) nanoparticles could be easily fabricated in EM- $\text{H}_2\text{O}$  solution in the presence of HMT at room temperature.

## 2. Experimental

### 2.1. Materials preparation

All chemical reagents were purchased from Shanghai Sinopharm. Chemical Reagent Ltd. Co. and used without any further purification. Take the synthesis of  $\delta\text{-Bi}_2\text{O}_3$  nanosheets for an example. A typical procedure is as follows.  $\text{Bi}(\text{NO}_3)_3 \cdot 5\text{H}_2\text{O}$  (0.98 g; 2 mmol) was dissolved in EG (10 mL) with continuous stirring to give a clear solution (pH = 2). Then, HMT aqueous solution (1 M; 20 mL) was added to above solution and pH of the solution was at about 6. The solution changed blur after stirring for about 10 h. With further stirring for 80 h, the resulting white precipitate was

centrifuged, washed several times with distilled water and ethanol, and then dried under vacuum at 60 °C for 10 h.

The other samples including  $\alpha$  and  $\beta$ -Bi<sub>2</sub>O<sub>3</sub>, BiON and Bi<sub>5</sub>O<sub>7</sub>NO<sub>3</sub> were obtained under identical conditions by varying the solvent to EM-H<sub>2</sub>O or pure H<sub>2</sub>O and the base to NaOH or NH<sub>3</sub> H<sub>2</sub>O. The pH of the mixed solution was adjusted by base variety and amount. Herein, EM and EG was separately used as a solvent to dissolve Bi(NO<sub>3</sub>)<sub>3</sub> · 5H<sub>2</sub>O because EG could act as a ligand as well as a solvent as comparison with EM. All the experimental parameters are listed in Table 1.

If the products prepared from above solution route were amorphous, they were successively calcined in air for 2 h at different temperatures ranging from 300 to 400 °C depending on the nature of the precursors (heating rate: 4 °C min<sup>-1</sup>).

## 2.2. Characterization

X-ray powder diffraction patterns (XRD) were obtained on a BRUKER D8 Advance X-ray diffractometer (Cu K $\alpha$  radiation,  $\lambda = 1.542 \text{ \AA}$ ) at a scan rate of 0.05 ° 2 $\theta$  s<sup>-1</sup>. Transmission electron microscopy (TEM) and field-emission scanning electron microscopy (FESEM) were carried out on a JEOL JEM-2100 and HITACHI S-4800 microscope, respectively. Brunauer-Emmett-Teller (BET) specific surface areas were analyzed based on nitrogen adsorption-desorption isotherm on a ASAP 2020 apparatus. All the samples were degassed at 200 °C prior to nitrogen adsorption measurements. X-ray photoelectron spectroscopy (XPS) measurements were carried out on a PHI Quantera II SXM X-ray photoelectron spectrometer with monochromatized Al K $\alpha$  as the exciting source, and the results obtained in the XPS

analysis were corrected by referencing the C 1s line to 284.8 eV. The UV-Vis diffuse reflectance spectra (DRS) of the products were recorded on a SHIMADZU UV 2550 spectrophotometer using BaSO<sub>4</sub> as a reference, and were converted from reflection to absorbance by the Kubelka-Munk method.

### 2.3. Photocatalytic activity test

The photocatalytic activity of the as-prepared samples was investigated by using RhB as a model compound. The photocatalytic reaction was performed in a XPA-7 photochemical reactor (Nanjing Xujiang Machine-electronic Company, China). In a typical photocatalytic experiment, 20 mg of photocatalyst was added into 50 mL of RhB solution (5 mg L<sup>-1</sup>). Prior to irradiation, the suspensions were stirred magnetically in the dark for 1 h to establish an adsorption-desorption equilibrium between the catalyst and dye, and then exposed to visible light (Xe lamp (500 W) with a 420 nm cutoff filter) under magnetic stirring. At a given time intervals, about 4 mL suspension was taken out and centrifuged at 8000 rpm for 15 min to remove the catalyst powders. The remnant RhB in the filtrate was determined with a UV-Vis spectrophotometer (BRAIC UV1201) by the maximum absorption at 554 nm.

## 3. Results and discussion

### 3.1. Phase and structures

The phase and composition of the samples synthesized under various experimental conditions were analyzed by XRD technique. XRD patterns indicate that the samples obtained from the reaction of Bi(NO<sub>3</sub>)<sub>3</sub> · 5H<sub>2</sub>O (2 mmol) and NH<sub>3</sub> · H<sub>2</sub>O (40 mmol; pH ≈ 9) or HMT (40 mmol; pH ≈ 6) in pure water were amorphous (Fig. S1a and b), which completely converted to yellow Bi<sub>5</sub>O<sub>7</sub>NO<sub>3</sub> (JCPDS No. 51-0525) after

calcination at 400 °C (Fig. 1a). No crystalline Bi<sub>2</sub>O<sub>3</sub> could be prepared even if the molar ratio of base/Bi(NO<sub>3</sub>)<sub>3</sub> was increased to 100 due to the weak basicity of NH<sub>3</sub> H<sub>2</sub>O and HMT.<sup>21</sup> Analogous to the reports,<sup>18,22</sup> NaOH as a base at a low (pH < 7) and high concentration (pH > 13) respectively induced the formation of basic bismuth nitrates and light yellow α-Bi<sub>2</sub>O<sub>3</sub> (Fig. S1c and d).

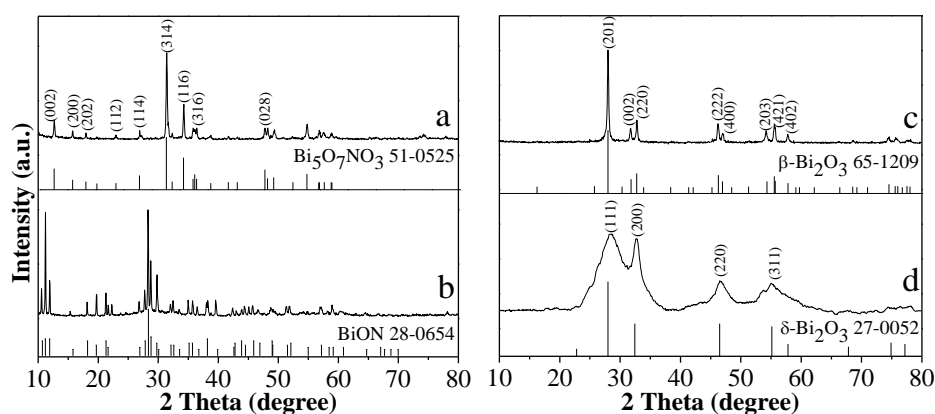


**Fig. 1.** XRD patterns of (a) Bi<sub>5</sub>O<sub>7</sub>NO<sub>3</sub>, (b) BiON, (c) β-Bi<sub>2</sub>O<sub>3</sub> and (d) δ-Bi<sub>2</sub>O<sub>3</sub>.

When EM was used as a solvent, Bi(NO<sub>3</sub>)<sub>3</sub> 5H<sub>2</sub>O could be completely dissolved in it. After aqueous HMT solution was added into above solution, phase pure BiON (JCPDS No. 28-0654) was produced when HMT amount varying from 2 to 40 mmol and pH accordingly ranging from 2.5 to 6 (Fig. 1b). The addition of a small amount of NH<sub>3</sub> H<sub>2</sub>O in place of HMT (pH < 7) also gave birth to a basic bismuth nitrate (Fig. S1e). However, if the amount of NH<sub>3</sub> H<sub>2</sub>O was increased to 40 mmol (pH ≈ 9), XRD demonstrated amorphous product, which converted to bright yellow β-Bi<sub>2</sub>O<sub>3</sub> (JCPDS No. 65-1209) after calcination at 350 °C for 2 h (Fig. 1c). Analogous to the case using pure water as a solvent, basic bismuth nitrates and α-Bi<sub>2</sub>O<sub>3</sub> were respectively formed at a low and high NaOH concentration (Fig. S1f). However, the morphologies of the products were different from each other to some extent, as discussed below.

If using EG as a solvent in place of EM, a mixture of basic bismuth nitrate and  $\delta$ - $\text{Bi}_2\text{O}_3$  with low crystallinity was formed at a low NaOH concentration ( $\text{pH} < 7$ ) (Fig. S1g). However, when NaOH concentration was increased to 40 mmol ( $\text{pH} > 13$ ), no precipitate appeared even with 90 h of stirring, which was quite different from the cases employing EM and pure water as solvents. Moreover, no product was formed after 90 h of reaction at a low HMT concentration (2 mmol,  $\text{pH} \approx 2.5$ ), whereas phase pure cubic  $\delta$ - $\text{Bi}_2\text{O}_3$  (JCPDS No. 27-0052) could be prepared by the addition of 40 mmol of HMT ( $\text{pH} \approx 6$ ) (Fig. 1d). In particular, the addition of a aqueous solution containing 40 mmol of  $\text{NH}_3 \cdot \text{H}_2\text{O}$  into  $\text{Bi}(\text{NO}_3)_3 \cdot 5\text{H}_2\text{O}/\text{EG}$  ( $\text{pH} \approx 9$ ) gave birth to tetragonal  $(\text{BiO})_2\text{CO}_3$  (JCPDS No. 41-1488) (Fig. S1h). While, if  $\text{NH}_3 \cdot \text{H}_2\text{O}$  amount was dropped to 2 mmol ( $\text{pH} \approx 6$ ), amorphous product was formed, which was transformed into tetragonal  $\beta$ - $\text{Bi}_2\text{O}_3$  by calcination at 300 °C for 2 h.

### 3.2. Formation mechanism

When  $\text{Bi}(\text{NO}_3)_3 \cdot 5\text{H}_2\text{O}$  was dispersed in pure water, it strongly hydrolyzed into white  $\text{BiONO}_3$ .<sup>23</sup> If a base was added into this solution,  $\text{BiONO}_3$  heterogeneously reacted with the base into various bismuth compounds, depending on the concentration and strength of the bases. The reaction of  $\text{BiONO}_3$  with a weak base like HMT and  $\text{NH}_3 \cdot \text{H}_2\text{O}$  resulted in the formation of amorphous products, whereas its reaction with a strong base like NaOH induced various bismuth compounds including basic bismuth nitrates and  $\alpha$ - $\text{Bi}_2\text{O}_3$ , depending NaOH concentration.<sup>18,22</sup>

When using EM to dissolve  $\text{Bi}(\text{NO}_3)_3 \cdot 5\text{H}_2\text{O}$ , the hydrolysis of  $\text{Bi}(\text{NO}_3)_3 \cdot 5\text{H}_2\text{O}$  could be restrained, which may help  $\text{Bi}^{3+}$  cations taking part in the reaction with a

base. Therefore, crystalline basic bismuth nitrate could be formed in the presence of HMT. The influence of a small amount of  $\text{NH}_3 \cdot \text{H}_2\text{O}$  on the product was similar to HMT due to identical pH range (2.5-6). Nevertheless, the addition of a large amount of  $\text{NH}_3 \cdot \text{H}_2\text{O}$  into  $\text{Bi}^{3+}/\text{EM}$  solution ( $\text{pH} \approx 9$ ) gave birth to amorphous product, and it converted to  $\beta\text{-Bi}_2\text{O}_3$  at  $350\text{ }^\circ\text{C}$ . While, the amorphous precursor obtained in pure water was transferred to  $\text{Bi}_5\text{O}_7\text{NO}_3$  at a calcination temperature up to  $400\text{ }^\circ\text{C}$ . As compared to EM, strong coordination interaction between EG and  $\text{Bi}^{3+}$  would slow down the release rate of  $\text{Bi}^{3+}$ , and subsequent reaction rate with a base. Therefore, no product was generated at a low HMT concentration. With HMT concentration increasing to above 20 mmol ( $\text{pH} \approx 6$ ), phase pure  $\delta\text{-Bi}_2\text{O}_3$  was generated. The formation of high-temperature phase  $\delta\text{-Bi}_2\text{O}_3$  may be due to coordination effect of EG, which plays a crucial role not only in the morphology, but also in phase transition of  $\text{Bi}_2\text{O}_3$ .<sup>24</sup> A strong base like NaOH may react with hydrogen atoms of hydroxyl group of EG, and thus intensified coordination ability of oxygen atoms with  $\text{Bi}^{3+}$ . As a consequence, no precipitate was formed at a high NaOH concentration (40 mmol; 1.3 M) in EG- $\text{H}_2\text{O}$  solution. The formation of  $(\text{BiO})_2\text{CO}_3$  at a high  $\text{NH}_3 \cdot \text{H}_2\text{O}$  concentration ( $\text{pH} \approx 9$ ) is not clear now and needs further investigation. At a low  $\text{NH}_3 \cdot \text{H}_2\text{O}$  concentration ( $\text{pH} \approx 6$ ), amorphous product was also obtained in EG- $\text{H}_2\text{O}$  solution, and it could be transferred into  $\beta\text{-Bi}_2\text{O}_3$  by calcining at  $300\text{ }^\circ\text{C}$ , lower than the case employing EM ( $350\text{ }^\circ\text{C}$ ) and  $\text{H}_2\text{O}$  ( $400\text{ }^\circ\text{C}$ ) as solvents. In addition, the decomposition temperature of the precursor  $\text{BiONO}_3$  obtained without the addition of any base reached as high as  $450\text{ }^\circ\text{C}$ . Usually, the decomposition temperature of

bismuth nitrate salts decreases with the atomic ratio of Bi:NO<sub>3</sub> increasing.<sup>2,13</sup> These results suggest that the reaction of NH<sub>3</sub> H<sub>2</sub>O with Bi<sup>3+</sup> cations (in EM solution) or Bi<sup>3+</sup>-EG complex (in EG solution) was faster than with BiONO<sub>3</sub> (in water solution), and therefore, the Bi:NO<sub>3</sub> ratio of the amorphous precursors increased due to the replacement of NO<sub>3</sub><sup>-</sup> by EG ligands and OH<sup>-</sup>. The nature of the bases and solvents exerts a great influence on the decomposition of the amorphous precursors. IR spectra of the precursor obtained in EG-H<sub>2</sub>O solution display the peaks at 879.6 and 1041.6 cm<sup>-1</sup>, which can be ascribed to C-H and C-O bond vibration (Fig. S2), respectively. This further demonstrates that coordination interaction existed between EG and Bi<sup>3+</sup>, which lowered the decomposition temperature of the precursor.

### 3.3. Morphology and composition

Electron microscope technology was used to check the morphology and size of the as-prepared samples. TEM and SEM images of BiON prepared in the presence of HMT in EM-H<sub>2</sub>O solution (pH = 2.5-6) illustrate distorted hexagonal prisms with a size of ca. 5 μm (Fig. 2a and inset). The typical TEM and SEM images of δ-Bi<sub>2</sub>O<sub>3</sub> obtained in the presence of HMT in EG-H<sub>2</sub>O solution (pH ≈ 6) reveal an aggregation of thin sheet clusters. The nanosheets are very thin with a thickness of about 15 nm and therefore relatively transparent to the electron beam (Fig. 2b and inset). The amorphous product prepared in ammonia aqueous solution is composed of uniform nanotubes with a diameter of about 5 nm and length in the range of 30 to 60 nm (Fig. S3a), which could convert to plate-like Bi<sub>5</sub>O<sub>7</sub>NO<sub>3</sub> by calcination at 400 °C (Fig. 2c and inset). β-Bi<sub>2</sub>O<sub>3</sub> prepared through solution crystallization in NH<sub>3</sub> H<sub>2</sub>O/EG-H<sub>2</sub>O

(pH  $\approx$  6) and subsequent calcination at 300  $^{\circ}$ C illustrates its irregular spherical nanoparticles with an average diameter of 0.5  $\mu$ m (Fig. 2d).  $(\text{BiO})_2\text{CO}_3$  obtained in  $\text{NH}_3 \text{H}_2\text{O}/\text{EG}-\text{H}_2\text{O}$  solution (pH  $\approx$  9) demonstrates its sheet-like morphology (Fig. S3b), which should be induced by its intrinsic layered structure characteristics. As discussed above, the heterogeneous reaction between  $\text{BiONO}_3$  and  $\text{NaOH}$  in pure water should be slower than homogeneous ones between  $\text{Bi}^{3+}$  and  $\text{NaOH}$  in  $\text{EM}-\text{H}_2\text{O}$  solution, and therefore,  $\alpha\text{-Bi}_2\text{O}_3$  nanoparticles prepared in  $\text{H}_2\text{O}$  and  $\text{EM}-\text{H}_2\text{O}$  solution with the same  $\text{NaOH}$  concentration respectively take on dendritic and diamond-like appearance due to various nucleation and growth rate (Fig. S3c and d).

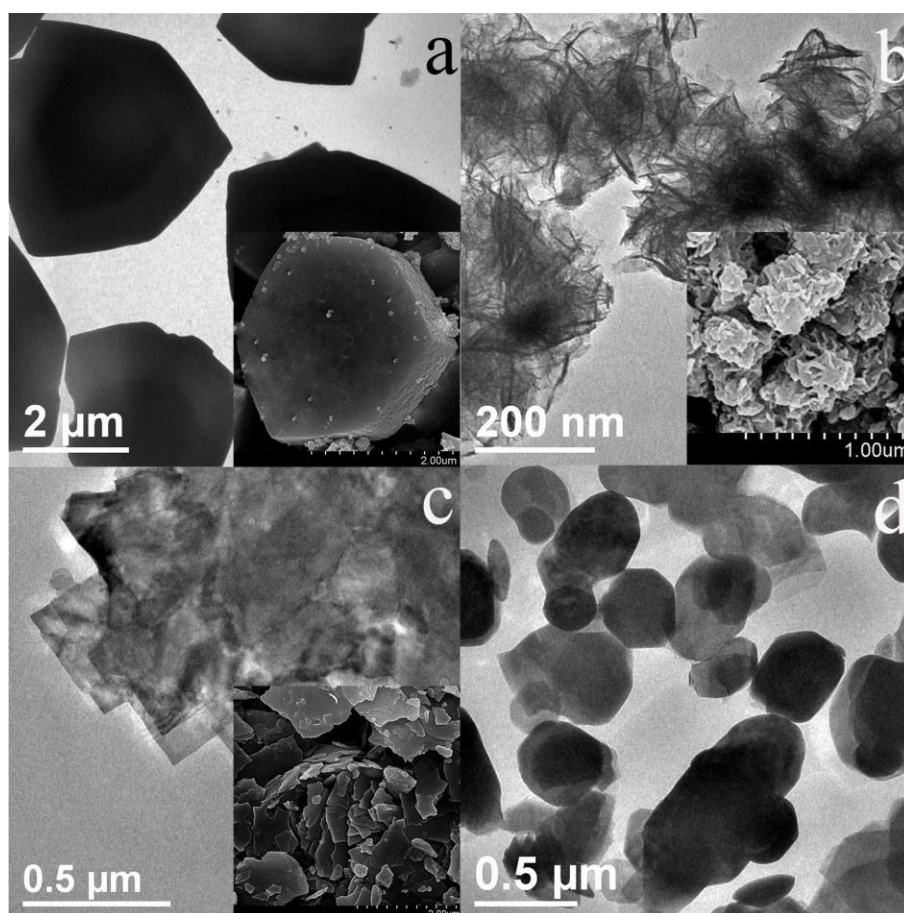


**Fig. 2.** TEM images of (a)  $\text{BiON}$ , (b)  $\delta\text{-Bi}_2\text{O}_3$ , (c)  $\text{Bi}_5\text{O}_7\text{NO}_3$  and (d)  $\beta\text{-Bi}_2\text{O}_3$ ; the insets in (a), (b) and (c) are their SEM images.

The phase and morphology of the as-prepared bismuth-based compounds are summarized in Table 1.

**Table 1.** Phase and morphology of the as-prepared samples through solution crystallization and subsequent calcination at <sup>a</sup> 300, <sup>b</sup> 350, and <sup>c</sup> 400 °C, respectively.

Solvent	Base (pH)	Product	Morphology
EG-H <sub>2</sub> O	HMT (6)	$\delta$ -Bi <sub>2</sub> O <sub>3</sub>	thin sheets
EG-H <sub>2</sub> O	NH <sub>3</sub> ·H <sub>2</sub> O (9)	Bi <sub>2</sub> O <sub>2</sub> CO <sub>3</sub>	sheet-based flowers
EG-H <sub>2</sub> O	<sup>a</sup> NH <sub>3</sub> ·H <sub>2</sub> O (6)	$\beta$ -Bi <sub>2</sub> O <sub>3</sub>	nanoparticles
EM-H <sub>2</sub> O	HMT (2.5-6)	BiON	hexagonal prisms
EM-H <sub>2</sub> O	NaOH (> 13)	$\alpha$ -Bi <sub>2</sub> O <sub>3</sub>	diamonds
EM-H <sub>2</sub> O	<sup>b</sup> NH <sub>3</sub> ·H <sub>2</sub> O (9)	$\beta$ -Bi <sub>2</sub> O <sub>3</sub>	nanoparticles
H <sub>2</sub> O	NaOH (> 13)	$\alpha$ -Bi <sub>2</sub> O <sub>3</sub>	dendrites
H <sub>2</sub> O	<sup>c</sup> NH <sub>3</sub> ·H <sub>2</sub> O (9)	Bi <sub>5</sub> O <sub>7</sub> NO <sub>3</sub>	plates

The surface composition and chemical state of the as-prepared BiON, Bi<sub>5</sub>O<sub>7</sub>NO<sub>3</sub> and  $\delta$ -Bi<sub>2</sub>O<sub>3</sub> were analyzed by using XPS (Fig. 3). XPS survey spectra of the BiON and Bi<sub>5</sub>O<sub>7</sub>NO<sub>3</sub> show the presence of the elements Bi, N, O and C (Fig. 3aA and B), and meanwhile, Bi, O and C elements were detected in  $\delta$ -Bi<sub>2</sub>O<sub>3</sub>. The C peak should originate from adventitious carbon. The high-resolution XPS spectra of Bi 4f in BiON show two peaks at 159.1 and 164.5 eV, corresponding to Bi 4f<sub>7/2</sub> and 4f<sub>5/2</sub>, respectively, which is characteristic of Bi<sup>3+</sup> (Fig. 3bA).<sup>25</sup> The deconvolution of O 1s spectra in BiON indicate three contributions of oxygen atoms from Bi-O at 529.9 eV, NO<sub>3</sub><sup>-</sup> at 530.8 eV, and hydroxyl group or H<sub>2</sub>O at 532.2 eV (Fig. 3cA). XPS spectrum of N 1s core level shows a peak at 406.5 eV (Fig. 3dA), corresponding to the binding energy of nitrogen atom in the NO<sub>3</sub><sup>-</sup> anion. The high-resolution XPS spectra of Bi 4f, O 1s and N 1s regions of Bi<sub>5</sub>O<sub>7</sub>NO<sub>3</sub> sample are similar to those of BiON except for slight

deviation of peak centers due to different chemical states (Fig. 3B).<sup>26</sup> The XPS spectra of  $\delta$ - $\text{Bi}_2\text{O}_3$  agree well with the report (Fig. 3C).<sup>17</sup>

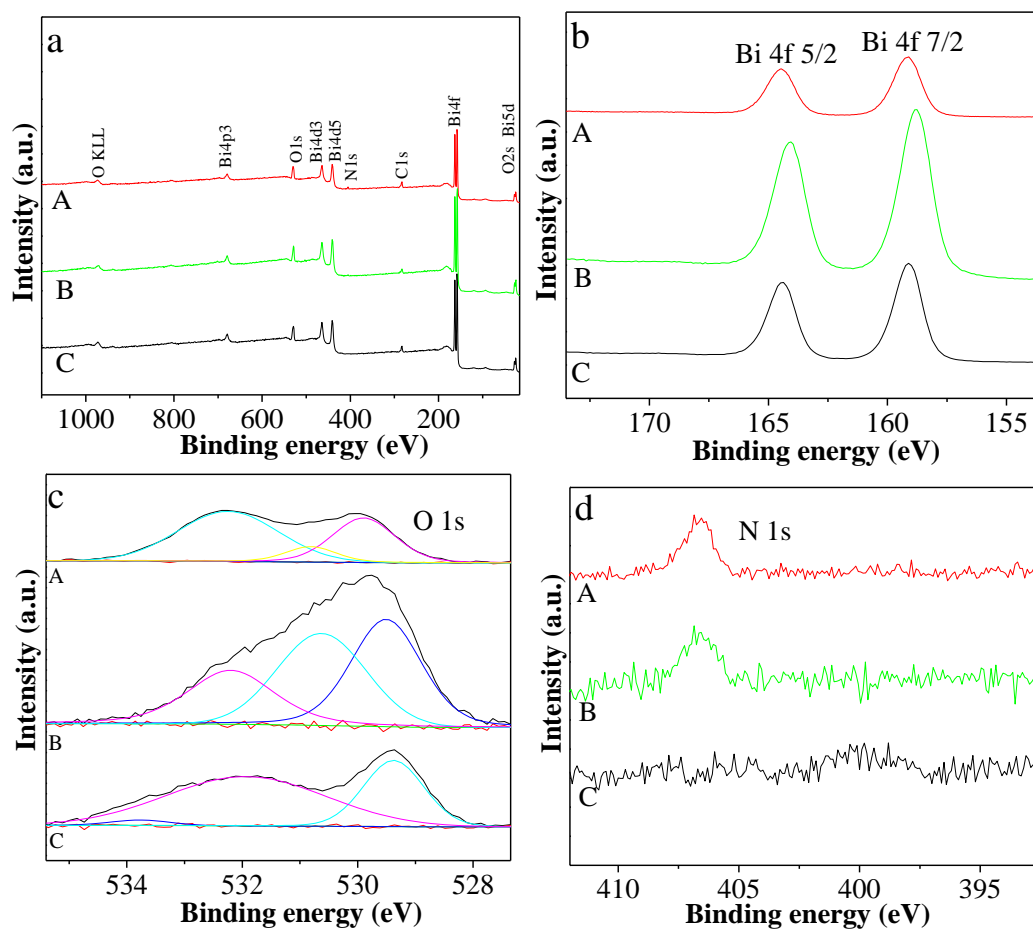


**Fig. 3.** XPS survey (a), Bi 4f (b), O 1s (c) and N 1s (d) spectra of the as-prepared samples: (A) BiON, (B)  $\text{Bi}_5\text{O}_7\text{NO}_3$  and (C)  $\delta$ - $\text{Bi}_2\text{O}_3$ .

### 3.4. Surface areas and pore size

The specific surface areas and pore size distribution are important factors to semiconducting materials in photocatalysis. The BET surface areas and pore size of the as-prepared  $\text{Bi}_2\text{O}_3$  nanoparticles of three polymorphic forms and plate-like  $\text{Bi}_5\text{O}_7\text{NO}_3$  were investigated by nitrogen adsorption/desorption isotherms. As shown in Fig. S4 and Table 2, all of the curves display typical type IV isotherms with H3

hysteresis loop, corresponding to slitlike pores from the aggregates of nanoplate or nanoparticles.  $\delta$ - $\text{Bi}_2\text{O}_3$  has the biggest hysteresis loop area (Fig. S4c), which is in agreement with its the highest surface area. The pore size distribution of  $\delta$ - $\text{Bi}_2\text{O}_3$  nanosheets is single-modal pattern with a peak centered at 20 nm (inset in Fig. S4c), which most likely arises from their inter-nanosheet spacings. The calculated mean pore diameter of  $\delta$ - $\text{Bi}_2\text{O}_3$  nanosheets is 23.23 nm from desorption branch of the nitrogen isotherm by the BJH (Barrett-Joyner-Halenda) method and BET surface area is  $23.67 \text{ m}^2 \text{ g}^{-1}$ , which are comparable to flower-like  $\delta$ - $\text{Bi}_2\text{O}_3$  synthesized by hydrothermal method.<sup>17</sup> The surface area of the as-prepared  $\text{Bi}_5\text{O}_7\text{NO}_3$  plates is higher than that of the reported sheet-like  $\text{Bi}_5\text{O}_7\text{NO}_3$ .<sup>27</sup>

**Table 2.** BET surface areas, pore volumes, mean pore diameters and band gap energy ( $E_g$ ) of the as-prepared  $\text{Bi}_2\text{O}_3$  and  $\text{Bi}_5\text{O}_7\text{NO}_3$ .

Sample	BET surf. areas ( $\text{m}^2 \text{ g}^{-1}$ )	Pore volumes ( $\text{cm}^3 \text{ g}^{-1}$ )	Mean pore diameters (nm)	$E_g$ (eV)
$\alpha$ - $\text{Bi}_2\text{O}_3$ <sup>a</sup>	1.28	0.0037	12.36	2.84
$\beta$ - $\text{Bi}_2\text{O}_3$	8.52	0.068	29.02	2.42
$\delta$ - $\text{Bi}_2\text{O}_3$	23.67	0.16	23.23	3.48
$\text{Bi}_5\text{O}_7\text{NO}_3$	8.51	0.051	24.73	2.51

<sup>a</sup> dendritic  $\alpha$ - $\text{Bi}_2\text{O}_3$ )

### 3.5. Optical properties

The optical absorption properties of the as-prepared bismuth nitrates and  $\text{Bi}_2\text{O}_3$  were studied by DRS spectra (Fig. 4). The maximal absorbance wavelength of  $\text{BiON}$  is around 373 nm with a band gap energy ( $E_g$ ) ca. 3.59 eV (Fig. 4a), indicating that it can only be irradiated by UV light. The  $\text{Bi}_5\text{O}_7\text{NO}_3$ ,  $\alpha$ -,  $\beta$ - and  $\delta$ - $\text{Bi}_2\text{O}_3$  reveal absorption edges at about 551, 458, 563 and 382 nm, which coincide with their yellow,

light yellow, orange yellow and white color, respectively, and the  $E_g$  values are approximately 2.51, 2.84, 2.42 and 3.48 eV, respectively (Fig. 4b-e), which were estimated from a plot of  $(\alpha h\nu)^2$  as a function of the photon energy ( $h\nu$ ) (inset of Fig. 4).

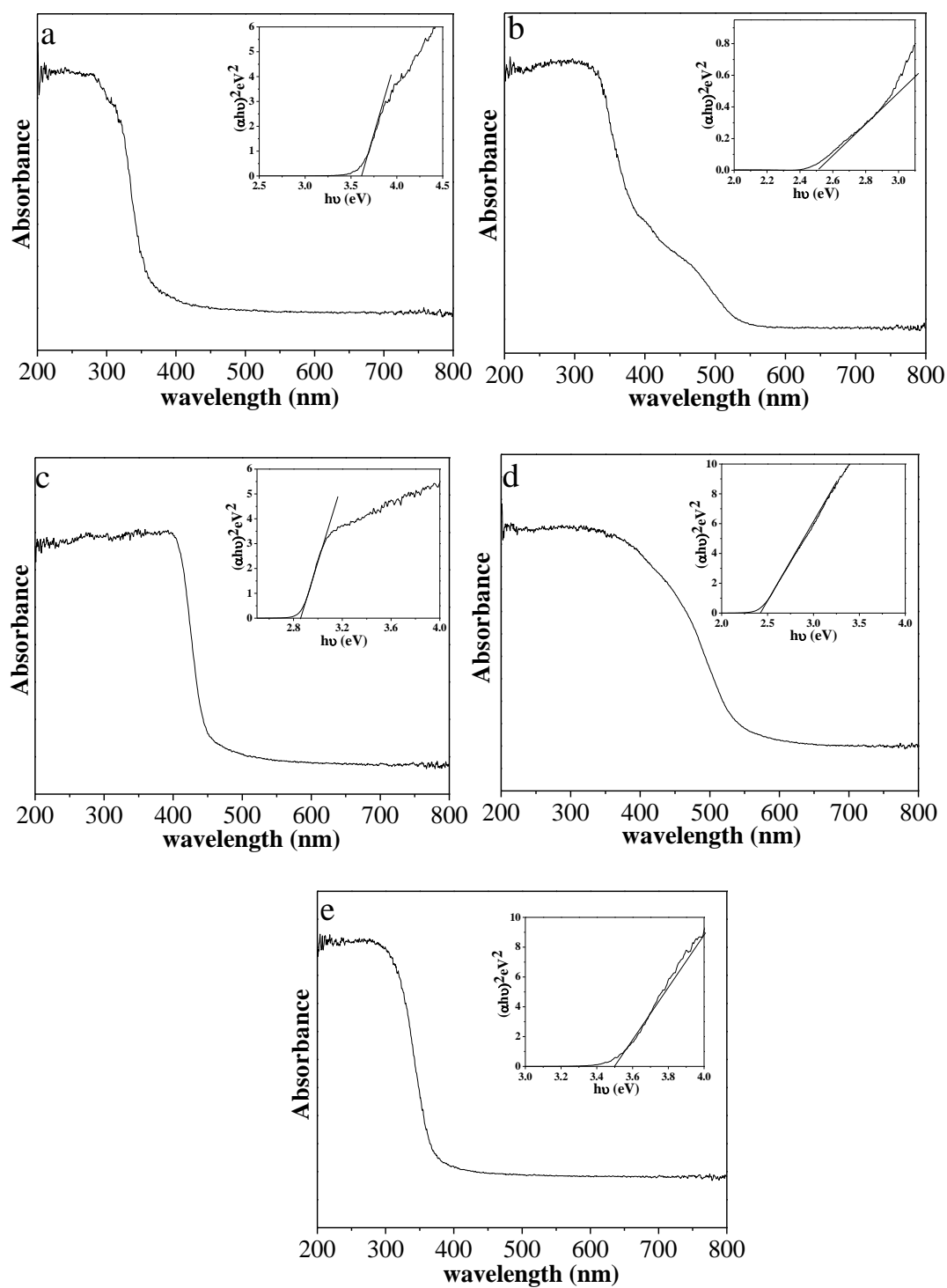


**Fig. 4.** DRS spectra and band gap energies (inset) of (a) BiON, (b)  $\text{Bi}_5\text{O}_7\text{NO}_3$ , (c)  $\alpha\text{-Bi}_2\text{O}_3$ , (d)  $\beta\text{-Bi}_2\text{O}_3$  and (e)  $\delta\text{-Bi}_2\text{O}_3$ .

### 3.6. Photocatalytic activity

Before photocatalytic activity measurement, we examined the adsorption properties of RhB over the as-prepared samples in the dark. As displayed in Fig. S5, the adsorption-desorption reached equilibrium about 20 min later over five samples. The  $\delta\text{-Bi}_2\text{O}_3$  nanosheets have most notable adsorptive ability for RhB of all the samples with a adsorptive efficiency of about 54%. The high adsorptive efficiency is related to its high surface area and large pore volume.

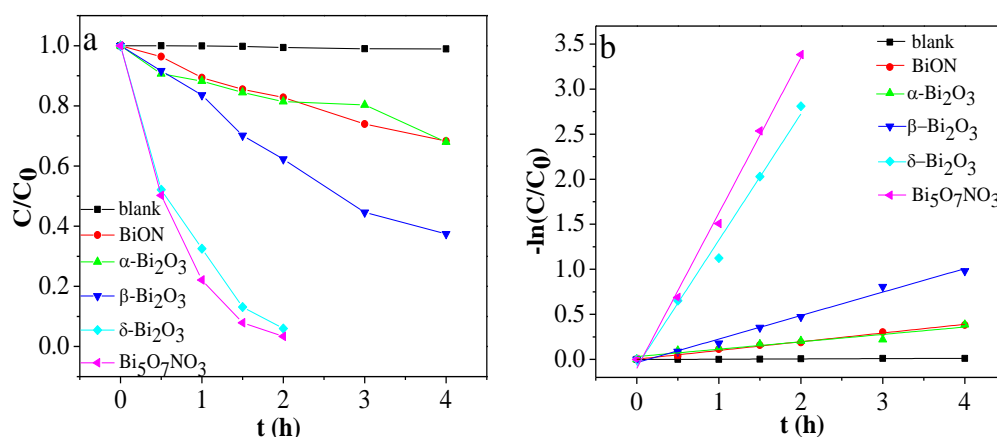


**Fig. 5.** (a) Degradation efficiency for RhB over the as-prepared  $\text{Bi}_2\text{O}_3$  and bismuth nitrates under visible light irradiation and (b) corresponding kinetic linear simulation curves.

The photocatalytic activity of the as-prepared samples was evaluated through degradation of RhB under visible light irradiation. Fig. 5a shows the photodegradation efficiency of RhB as a function of irradiation time over various photocatalysts, where  $C_0$  is the initial concentration of RhB after adsorption-desorption equilibration, and  $C$  is the concentration of RhB at different irradiation time, which was measured by UV-Vis spectrophotometer (Fig. S6). It can be seen that negligible photolysis of RhB occurred within 4 h of visible light irradiation without any photocatalyst (blank).

Fig. 5a also indicates that  $\delta$ - $\text{Bi}_2\text{O}_3$  nanosheets exhibit the highest photocatalytic activity for RhB decomposition of three kinds of  $\text{Bi}_2\text{O}_3$  polymorphs, and the degradation efficiency reaches 94% after 2 h compared to 19 and 38% for  $\alpha$ - $\text{Bi}_2\text{O}_3$  and  $\beta$ - $\text{Bi}_2\text{O}_3$ , respectively. These photocatalytic reactions fit well the pseudo-first-order kinetics model with apparent reaction rate constant ( $k$ ) 1.40, 0.26 and 0.082  $\text{h}^{-1}$  for  $\delta$ - $\text{Bi}_2\text{O}_3$ ,  $\beta$ - $\text{Bi}_2\text{O}_3$  and  $\alpha$ - $\text{Bi}_2\text{O}_3$ , respectively (Fig. 5b). The  $k$  values normalized by their surface areas ( $k'$ ) are 0.059, 0.031 and 0.064  $\text{g h}^{-1} \text{m}^{-2}$ , respectively. The  $k'$  value of  $\delta$ - $\text{Bi}_2\text{O}_3$  is a little smaller than that of  $\alpha$ - $\text{Bi}_2\text{O}_3$ , implying that the photocatalytic activity of  $\text{Bi}_2\text{O}_3$  mainly depends on their surface areas. Besides, in the presence of  $\delta$ - $\text{Bi}_2\text{O}_3$ , the maximal absorption peak of RhB at 554 nm slightly blue shifts and turns broadened and lowered with the irradiation time increasing, which indicates that RhB was photodegraded accompanied by a photosensitization process (Fig. S6c). The degradation experiment of colorless salicylic acid solution over  $\delta$ - $\text{Bi}_2\text{O}_3$  under identical condition to RhB displays slight degradation within 2 h (Fig. S7), further demonstrating an indirect dye photosensitization process. Although the degradation efficiency of RhB over the as-prepared  $\delta$ - $\text{Bi}_2\text{O}_3$  is just slightly higher than the reported  $\delta$ - $\text{Bi}_2\text{O}_3$  catalyst,<sup>16</sup> the catalyst dose herein (20 mg) is much smaller than the reported value (50 mg).

The durability of  $\delta$ - $\text{Bi}_2\text{O}_3$  nanosheets was evaluated by recycling the used catalyst. As shown in Fig. 6a, the decrease of the photocatalytic activity is less than 5% after four cycles, indicating the as-prepared  $\delta$ - $\text{Bi}_2\text{O}_3$  nanosheets possess favorable recycling characteristics under visible light illumination.

Reactive species experiments of  $\delta\text{-Bi}_2\text{O}_3$  indicate that the addition of IPA (isopropyl alcohol; a quencher of  $\bullet\text{OH}$  radical) did not significantly affected the photo-degradation activity of  $\delta\text{-Bi}_2\text{O}_3$  catalysts, which suggests that  $\bullet\text{OH}$  radicals was minor active species (Fig. 6b). While, the addition of BQ (benzoquinone; a quencher of  $\bullet\text{O}_2^-$ ) shows an inhibitory effect on the degradation of RhB to some extent, indicating that  $\bullet\text{O}_2^-$  is main active species. In particular, if AO (ammonium oxalate; a quencher of hole) was added into the system, the photo-degradation efficiency of RhB significantly decreased, implying that  $h^+$  is dominant reactive species in this photocatalytic system. The photo-induced holes could directly oxidize the adsorbed dye molecules, and thus high adsorption capacity benefits for its photocatalysis. In addition, RhB molecules adsorbed on the surface of  $\delta\text{-Bi}_2\text{O}_3$  nanosheets could be sensitized by visible light, and then an electron was transferred from the sensitized RhB molecule to conduction band (CB), which can be captured by  $\text{O}_2$  to generate  $\bullet\text{O}_2^-$ . Therefore, the photocatalytic process of  $\delta\text{-Bi}_2\text{O}_3$  was completed by both direct photoexcitation and indirect dye photosensitization. A small amount of  $\bullet\text{OH}$  radicals may result from the  $\bullet\text{O}_2^-$  radicals.

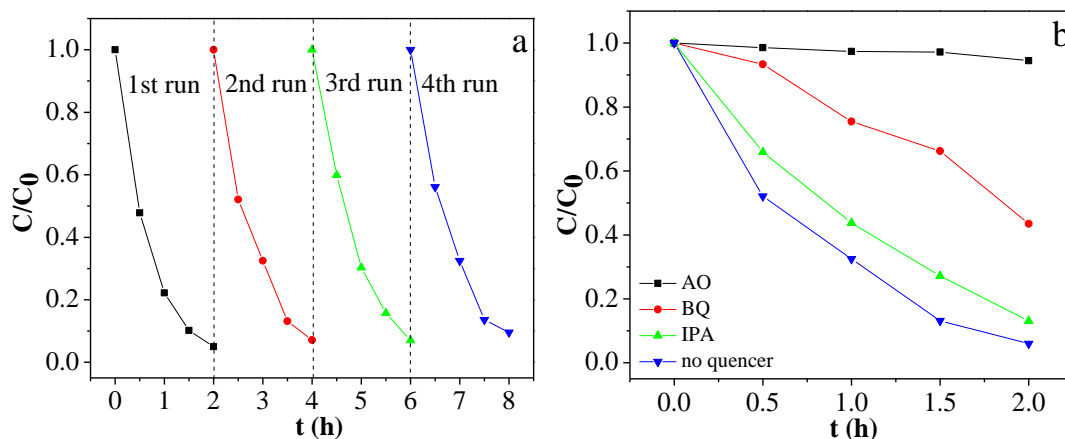


**Fig. 6.** (a) Recycling test and (b) time course of the photodegradation of RhB over  $\delta\text{-Bi}_2\text{O}_3$

catalyst under visible light irradiation in the presence of various quenchers (1 mM).

Considering that the tested RhB concentration was high in some literatures, the effect of the catalyst weight and initial RhB concentration on the photocatalytic activity of  $\delta$ -Bi<sub>2</sub>O<sub>3</sub> nanosheets have also been studied to explore the optimum photocatalytic reaction conditions. As displayed in Fig. 7a, the degradation efficiency increased with  $\delta$ -Bi<sub>2</sub>O<sub>3</sub> weight rising from 10 to 90 mg in 50 mL of RhB solution (20 mg L<sup>-1</sup>), which should be caused by the increment of the active centers. However, when the catalyst weight exceeded 90 mg, the degradation efficiency decreased instead, which may be due to the enhancement of light scattering and opacity.<sup>13</sup> The investigation of the influence of RhB initial concentration on degradation efficiency of  $\delta$ -Bi<sub>2</sub>O<sub>3</sub> (50 mg) indicates that the degradation efficiency monotonically decreased with RhB initial concentration increasing from 10 to 30 mg L<sup>-1</sup> (Fig. 7b). This could be rationalized by the masking effect of too much adsorbed RhB on the surface of catalyst, which may obstruct the transfer of light to the catalyst surface and thus impede the photoactivation process.<sup>28</sup>

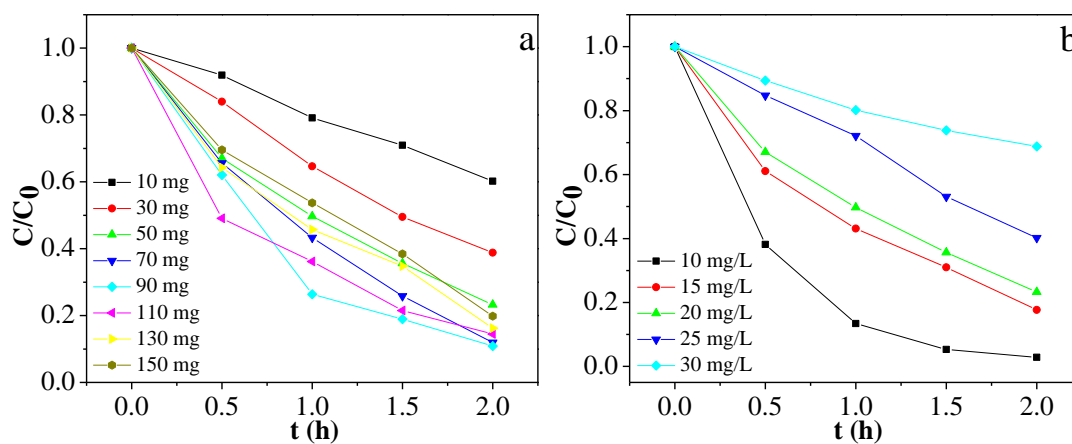


**Fig. 7.** Effect of (a) the catalyst weight and (b) initial RhB concentration on the photocatalytic activity of  $\delta$ -Bi<sub>2</sub>O<sub>3</sub> nanosheets, where the initial RhB concentration was kept at 20 mg L<sup>-1</sup> and catalyst weight was fixed to 50 mg for conditional experiments, respectively.

Fig. 5a shows that RhB could almost completely be degraded over the as-prepared Bi<sub>5</sub>O<sub>7</sub>NO<sub>3</sub> nanoplates within 2 h of visible light irradiation, which is comparable to Bi<sub>5</sub>O<sub>7</sub>NO<sub>3</sub> nanofibers prepared via Triton-assisted hydrothermal route,<sup>26</sup> but lower than Bi<sub>5</sub>O<sub>7</sub>NO<sub>3</sub> nanosheets obtained by hydrothermal method.<sup>27</sup> Nevertheless, the synthetic process of Bi<sub>5</sub>O<sub>7</sub>NO<sub>3</sub> in this work is simple. Furthermore, Bi<sub>5</sub>O<sub>7</sub>NO<sub>3</sub> nanoplates herein possess high photostability (Fig. S8).

There are few reports on the photocatalytic activity of basic bismuth nitrates. Liu et al prepared Bi<sub>6</sub>O<sub>6</sub>(OH)<sub>3</sub>(NO<sub>3</sub>)<sub>3</sub>·1.5H<sub>2</sub>O via a microwave-hydrothermal process and demonstrated its UV light driven activity for MO degradation.<sup>29</sup> Although visible-light-induced photocatalytic activity of the as-prepared BiON is low due to its large band gap energy (3.59 eV) (Fig. 5a), it exhibited enhanced degradation efficiency for MO under UV light irradiation as compared to Liu's work (Fig. S9).<sup>29</sup>

#### 4. Conclusions

Controlled experiments were systematically conducted to investigate the influence of the bases (pH) and solvents on the information of bismuth oxides from Bi(NO<sub>3</sub>)<sub>3</sub>·5H<sub>2</sub>O. Except for conventionally reported  $\alpha$ -Bi<sub>2</sub>O<sub>3</sub>,  $\delta$ -Bi<sub>2</sub>O<sub>3</sub> nanosheets have been synthesized in the presence of HMT in EG-H<sub>2</sub>O solution (pH  $\approx$  6) at room temperature. Spherical  $\beta$ -Bi<sub>2</sub>O<sub>3</sub> could be fabricated through calcining the precursor obtained in the presence of NH<sub>3</sub>·H<sub>2</sub>O in EG-H<sub>2</sub>O (pH  $\approx$  6) or EM-H<sub>2</sub>O (pH  $\approx$  9)

solution, whereas, the calcination for the precursor prepared in aqueous ammonia solution (pH  $\approx$  9) gave birth to  $\text{Bi}_5\text{O}_7\text{NO}_3$  nanoplates. Uniform  $\text{Bi}_6\text{O}_6(\text{OH})_2(\text{NO}_3)_4 \cdot 2\text{H}_2\text{O}$  prisms were formed in HMT/EM- $\text{H}_2\text{O}$  solution (pH range 2.5-6). Generally speaking, the reaction between  $\text{BiONO}_3$  from the hydrolysis of  $\text{Bi}(\text{NO}_3)_3 \cdot 5\text{H}_2\text{O}$  and a base in  $\text{H}_2\text{O}$  gave birth to bismuth-based compounds with various Bi: $\text{NO}_3$  ratio, depending on the basicity, and while, EM or EG as a solvent instead of  $\text{H}_2\text{O}$  could prohibit the hydrolysis of  $\text{Bi}(\text{NO}_3)_3 \cdot 5\text{H}_2\text{O}$ , thus releasing free  $\text{Bi}^{3+}$  cations or  $\text{Bi}^{3+}$ -EG complexes, which induced various products when reacted with a base, dependent on the base and solvent varieties. The as-prepared  $\delta$ - $\text{Bi}_2\text{O}_3$  and  $\text{Bi}_5\text{O}_7\text{NO}_3$  exhibited good photocatalytic activity for RhB degradation under visible light irradiation owing to their sheet or plate-like morphology, high surface areas and strong adsorptive ability for RhB.

### Acknowledgments

The work is financially supported by the National Natural Science Foundation of China (51372117 and 51322212), and the Natural Science Foundation of Jiangsu Province (BK20131347).

### Notes and references

\* *Key Laboratory for Soft Chemistry and Functional Materials, Ministry of Education, Nanjing University of Science and Technology, Nanjing 210094, China*

*E-mail: [hanqiaofeng@njust.edu.cn](mailto:hanqiaofeng@njust.edu.cn); [zhujw@njust.edu.cn](mailto:zhujw@njust.edu.cn)*

† Electronic supplementary information (ESI) available: XRD patterns, FTIR spectrum, TEM images, nitrogen adsorption-desorption isotherms of the as-prepared samples, and UV-Vis spectral changes of RhB with irradiation time. See DOI:

- 1 Q. Q. Huang, S. N. Zhang, C. X. Cai and B. Zhou, *Mater. Lett.*, 2011, 65, 988-990.
- 2 J. L. Wang, X. D. Yang, K. Zhao, P. F. Xu, L. B. Zong, R. B. Yu, D. Wang, J. X. Deng, J. Chen and X. R. Xing, *J. Mater. Chem. A*, 2013, 1, 9069-9074.
- 3 J. Li, Y. Yu and L. Z. Zhang, *Nanoscale*, 2014, 6, 8473-8488.
- 4 Q. Y. Li, H. T. Liu, F. Dong and M. Fu, *J. Colloid Interface Sci.*, 2013, 408, 33-42.
- 5 S. Q. Xia and S. Bobev, *Chem. Mater.*, 2010, 22, 840-850.
- 6 A. Cabot, A. Marsal, J. Arbiol and J. R. Morante, *Sens. Actuators, B*, 2004, 99, 74-89.
- 7 D. D. Zhang, S. M. Eaton, Y. Yu, L. T. Dou and P. D. Yang, *J. Am. Chem. Soc.*, 2015, 137, 9230-9233.
- 8 Y. Q. Wu and G. X. Lu, *Phys. Chem. Chem. Phys.*, 2014, 16, 4165-4175.
- 9 Y. Wang, J. Z. Zhao, B. Zhou, Z. C. Wang and Y. C. Zhu, *J. Alloys Compd.*, 2014, 592, 296-300.
- 10 L. L. Yang, Q. F. Han, J. Zhao, J. W. Zhu, X. Wang and W. H. Ma, *J. Alloys Compd.*, 2014, 614, 353-359.
- 11 J. L. Wang, X. D. Yang, K. Zhao, P. F. Xu, L. B. Zong, R. B. Yu, D. Wang, J. X. Deng, J. Chen and X. R. Xing, *J. Mater. Chem. A*, 2013, 1, 9069-9074.
- 12 X. Xiao, R. P. Hu, C. Liu, C. L. Xing, C. Qian, X. X. Zuo, J. M. Nan and L. S. Wang, *Appl. Catal. B Environ.*, 2013, 140-141, 433-443.
- 13 R. P. Hu, X. Xiao, S. H. Tu, X. X. Zuo and J. M. Nan, *Appl. Catal. B Environ.*, 2015, 163, 510-519.
- 14 F. Qin, G. F. Li, R. M. Wang, J. L. Wu, H. Z. Sun and R. Chen, *Chem. Eur. J.*, 2012, 18, 16491-16497.

- 15 B. J. Yang, M. S. Mo, H. M. Hu, C. Li, X. G. Yang, Q. W. Li and Y. T. Qian, *Eur. J. Inorg. Chem.*, 2004, 1785-1787.
- 16 L. Zhou, W. Z. Wang, H. L. Xu, S. M. Sun and M. Shang, *Chem. Eur. J.*, 2009, 15, 1776-1782.
- 17 L. Liu, W. Liu, X. L. Zhao, D. M. Chen, R. S. Cai, W. Y. Yang, S. Komarneni and D. J. Yang, *ACS Appl. Mater. Interface*, 2014, 6, 16082-16090.
- 18 A. N. Christensen, M.-A. Chevallier, J. Skibsted and B. B. Iversen, *J. Chem. Soc., Dalton Trans.*, 2000, 265-270.
- 19 G. Hägg, *General and Inorganic Chemistry*, John Wiley & Sons, Inc., New York, 1969, p. 580.
- 20 L. Y. Xie, J. X. Wang, Y. H. Hu, S. Y. Zhu, Z. Y. Zheng, S. X. Weng and P. Liu, *RSC Adv.*, 2012, 2, 9881-9886.
- 21 Y. Xiang, H. Y. Chen, H. S. Huh and S. W. Lee, *J. Solid State Chem.*, 2007, 180, 2510-2516.
- 22 Y. C. Wu, Y. C. Chang, C. Y. Huang, S. F. Wang and H. Y. Yang, *Dyes and Pigments*, 2013, 98, 25-30.
- 23 A. Kudo, K. Omori and H. Kato, *J. Am. Chem. Soc.*, 1999, 121, 11459-11467.
- 24 Y. Wang and Y. L. Li, *J. Colloid Interface Sci.*, 2015, 454, 238-244.
- 25 Č. Jovalekić, M. Pavlović, P. Osmokrović and L. Atanasoska, *Appl. Phys. Lett.*, 1998, 72, 1051-1053.
- 26 S. J. Yu, G. K. Zhang, Y. Y. Gao and B. B. Huang, *J. Colloid Interface Sci.*, 2013, 15, 322-330.
- 27 L. Z. Zhang, L. J. Chou and X. H. Li, *CrystEngComm*, 2013, 15, 10579-10583.
- 28 H. Gnayem and Y. Sasson, *ACS Catal.*, 2013, 3, 186-191.

29 L. Y. Xie, J. X. Wang, Y. H. Hu, Z. Y. Zheng, S. X. Weng, P. Liu, X. C. Shi and D. H. Wang,

*Mater. Chem. Phys.*, 2012, 136, 309-312.

## Figure captions

**Fig. 1.** XRD patterns of (a)  $\text{Bi}_5\text{O}_7\text{NO}_3$ , (b)  $\text{BiON}$ , (c)  $\beta\text{-Bi}_2\text{O}_3$  and (d)  $\delta\text{-Bi}_2\text{O}_3$ .

**Fig. 2.** TEM images of (a)  $\text{BiON}$ , (b)  $\delta\text{-Bi}_2\text{O}_3$ , (c)  $\text{Bi}_5\text{O}_7\text{NO}_3$  and (d)  $\beta\text{-Bi}_2\text{O}_3$ ; the insets in (a), (b) and (c) are their SEM images.

**Fig. 3.** XPS survey (a), Bi 4f (b), O 1s (c) and N 1s (d) spectra of the as-prepared samples: (A)  $\text{BiON}$ , (B)  $\text{Bi}_5\text{O}_7\text{NO}_3$  and (C)  $\delta\text{-Bi}_2\text{O}_3$ .

**Fig. 4.** DRS spectra and bandgap energies (inset) of (a)  $\text{BiON}$ , (b)  $\text{Bi}_5\text{O}_7\text{NO}_3$ , (c)  $\alpha\text{-Bi}_2\text{O}_3$ , (d)  $\beta\text{-Bi}_2\text{O}_3$  and (e)  $\delta\text{-Bi}_2\text{O}_3$ .

**Fig. 5.** (a) Degradation efficiency for RhB over the as-prepared  $\text{Bi}_2\text{O}_3$  and bismuth nitrates under visible light irradiation and (b) corresponding kinetic linear simulation curves.

**Fig. 6.** (a) Recycling test and (b) time course of the photodegradation of RhB over  $\delta\text{-Bi}_2\text{O}_3$  catalyst under visible light irradiation in the presence of various quenchers (1 mM).

**Fig. 7.** Effect of (a) the catalyst weight and (b) initial RhB concentration on the photocatalytic activity of  $\delta\text{-Bi}_2\text{O}_3$  nanosheets, where the initial RhB concentration was kept at  $20 \text{ mg L}^{-1}$  and catalyst weight was fixed to 50 mg for conditional experiments, respectively.

**Table 1.** Phase and morphology of the as-prepared samples through solution crystallization and subsequent calcination at <sup>a</sup> 300, <sup>b</sup> 350, and <sup>c</sup> 400 °C, respectively.

**Table 2.** BET surface areas, pore volumes, mean pore diameters and  $E_g$  of the as-prepared  $\text{Bi}_2\text{O}_3$  and  $\text{Bi}_5\text{O}_7\text{NO}_3$ .

A table of content:

## Controlled synthesis of bismuth-containing compounds ( $\alpha$ , $\beta$ and $\delta$ - $\text{Bi}_2\text{O}_3$ , $\text{Bi}_5\text{O}_7\text{NO}_3$ and $\text{Bi}_6\text{O}_6(\text{OH})_2(\text{NO}_3)_4 \cdot 2\text{H}_2\text{O}$ ) and their photocatalytic performance

Shu Gong, Qiaofeng Han\*, Xin Wang, and Junwu Zhu\*

A series of bismuth-containing compounds including  $\alpha$ ,  $\beta$  and  $\delta$ - $\text{Bi}_2\text{O}_3$ ,  $\text{Bi}_5\text{O}_7\text{NO}_3$  and  $\text{Bi}_6\text{O}_6(\text{OH})_2(\text{NO}_3)_4 \cdot 2\text{H}_2\text{O}$  could be easily prepared by changing the base and solvent variety.

